

The effect of roughness and residual stresses on fatigue life time of an alloy of titanium

K. Moussaoui · M. Mousseigne · J. Senatore ·
R. Chieragatti

Received: 19 May 2014 / Accepted: 16 November 2014 / Published online: 10 December 2014
© Springer-Verlag London 2014

Abstract The quality of titanium alloy parts in the aeronautical field demands great reliability, especially in fatigue resistance. This is mainly determined by surface integrity, which is in turn defined by geometrical, mechanical and metallurgical parameters. The present article provides a study of the influence that surface integrity has on the fatigue life of Ti6Al4V. Milling plans of procedure generating widely varying surface integrities were performed on fatigue test coupons. Four-point bending tests were then conducted. No influence of the geometric and metallurgical parameters was observed. Only the mechanical parameter seems to have a preponderant influence on fatigue life.

Keywords Surface integrity · Residual stress · Ti6Al4V · Fatigue life

1 Introduction

Fatigue is one of the main causes of damage to aviation structures. It is produced when a cyclical variation in mechanical stress appears, for example during the stages of flight of an aircraft. The fatigue phenomenon is characterised by three phases: the initiation of cracks, their propagation and then final failure. Examination of the fracture morphology shows that in most cases, crack initiation starts on the surface and persistence of the crack then represents

90 % of the part's lifetime [1]. The surface integrity of parts thus plays a major role in fatigue behaviour. The surface integrity properties of a part can be significantly modified by the manufacturing process, especially machining. This is generally defined by three parameters:

- the geometric parameter: roughness
- the mechanical parameter: residual stresses
- the metallurgical parameter: the microstructure and microhardness

The present study focuses on Ti6Al4V, a titanium alloy widely used in the aeronautical field, especially for applications requiring excellent mechanical resistance at high temperature. Titanium alloys have a density 40 % lower than steels and excellent resistance to corrosion. However, these alloys are also known to be difficult materials to machine. This is due to their strong mechanical resistance at high temperatures, a relatively low modulus of elasticity, low thermal conductivity and strong chemical reactivity [2–5]. The quality of titanium alloy parts in the aviation field requires great reliability, especially in terms of fatigue lifetime, which is largely dependent on surface integrity.

This article is part of a more general study on the influence of machining on the fatigue lifetime of titanium alloy aviation parts. The study itself is broken down into two stages covering firstly the influence of machining on surface integrity and secondly the influence of surface integrity on fatigue lifetime. This article investigates this second stage. A review of the literature follows.

Novovic et al. provide a bibliographical study on the effect of machining and surface integrity of the part on the fatigue lifetime of parts for various materials, including especially titanium alloys [1]. Novovic et al. provide a

K. Moussaoui (✉) · M. Mousseigne · J. Senatore · R. Chieragatti
Universit de Toulouse 3 - Paul Sabatier, 118 Route de Narbonne,
31062 Toulouse, France
e-mail: kamel.moussaoui@univ-tlse3.fr

bibliographical study on the effect of machining and surface integrity of the part on the fatigue lifetime of parts for various materials, particularly titanium alloys. Despite some discordant voices in the bibliography, the authors report that, in most cases, some lower levels of surface roughness lead to a better fatigue lifetime. In the domain of long lifetimes, initiation of the crack constitutes 90 % of the part's fatigue lifetime. In the absence of residual stresses, the roughness of the machined surfaces showing a roughness R_a greater than $0.1 \mu\text{m}$ has a major influence on fatigue resistance. Conversely (for surfaces machined with $R_a < 0.1 \mu\text{m}$), the roughness of the milled surface seems to have a lesser effect on fatigue resistance. It can be seen that the cracks initiate either due to persistent slip bands or at the joints of grains. Finally, if the microstructure shows inclusions of size greater than the surface roughness, it is inclusions that will determine fatigue resistance rather than roughness. Other studies have also shown the influence of roughness on the fatigue lifetime, especially when it comes to crack initiation [6, 7]. However, roughness cannot alone explain the part's fatigue behaviour [8]. Machining operations generate surface roughness or surface defects but also residual stresses and hardening in the upper layer. These parameters can influence the fatigue lifetime.

Residual stresses (RS) have generally been recognised as one of the most influential surface condition factors on a part's performance, especially on fatigue lifetime. It is essential to take residual stresses into account in many cases of fatigue. The generation of residual tensile stresses in a part can have negative consequences on fatigue resistance and conversely, residual compression stresses can considerably improve fatigue resistance [9–13]. Residual compression stresses can delay crack propagation [14–17]. The residual stresses in the part are defined by a profile that is usually characterised by the residual stress on the surface and the maximum residual stress in the thickness of the part. It is thus difficult to determine which of these two stresses has the greater influence on fatigue lifetime [18]. The beneficial effect of residual compression stresses on the fatigue lifetime is established. However, they can diminish to the point of disappearing by relaxation. This relaxation can be produced for fatigue tests conducted at high temperature or when the stresses imposed generate a plastic deformation. As stated in the bibliography, machining also generates work hardening of the superficial layer.

Specifically, a fine equiaxial microstructure (fine grains) leads to an increase in fatigue resistance in a vacuum. Conversely, for fatigue resistance in air, a bimodal microstructure is the most effective but it has small α grains of about $6 \mu\text{m}$. Lamellar microstructures are the least effective. The oxygen content of titanium alloy also plays a role in fatigue resistance. Indeed, the more oxygen there is the better fatigue resistance will be. The levels of oxygen influence

precipitation and hardening mechanisms, thus improving resistance to dislocations and improving fatigue resistance [19]. Speed of crack propagation lamellar microstructure provides the best results. It reduces the crack propagation speed as it increases the tortuosity of the structure [20]. In the case of crack initiation on the surface, a high density of dislocation or hardening causes an improvement in the fatigue lifetime by delaying initiation of cracks but accelerates their propagation [16]. In conclusion, hardening of the superficial layer makes initiation of cracks (90 % of the lifetime) more difficult and thus improves fatigue resistance of the parts. However, due to the fact that hardening reduces ductility, the crack propagation speed is increased. Finally, the microstructure of the superficial layer is also an influential factor in fatigue resistance. This study addresses this gap.

A number of studies have shown that fatigue lifetime is strongly influenced by the integrity of the surface as described by geometric, mechanical and metallurgical parameters. However, it is difficult to separate the respective influence of each of these parameters due to their combined effect. Most studies conclude that geometric defects have a negative effect on the lifetime. Meanwhile, residual stresses are extremely beneficial as they delay propagation of cracks when they are in compression, especially in the case where surface treatments such as peening are applied. As for the increase in hardening, it tends to improve resistance to crack initiation on the surface and reduce resistance to crack propagation. Nevertheless, few studies can be noted relating to the material under consideration (Ti6Al4V) that connect surface integrity with fatigue lifetime. In particular, consideration for all the surface integrity parameters (geometrical, mechanical and metallurgical) appears to be lacking.

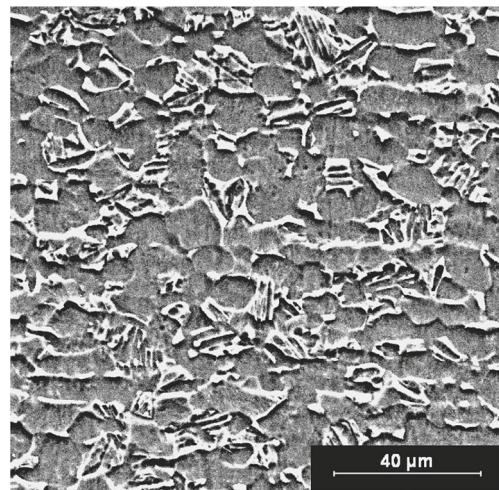


Fig. 1 Microstructure of Ti6Al4V alloy studied

Table 1 Nominal chemical composition of Ti6Al4V alloy (AFNOR L14-601)

Elément	Ti	Al	V	Fe	O	C	N	H
% weight	Base	5.5 – 6.75	3.5 – 4.5	< 0.25	< 0.2	< 0.08	< 0.05	< 0.01

2 Material and methods

2.1 Material

The material studied is an $\alpha + \beta$ two-phase titanium alloy, Ti6Al4V. It is received in the form of plates that are obtained by hot rolling and followed by annealing heat treatment. Figure 1 shows the bimodal or duplex $\alpha + \beta$ microstructure. Phase α is shown in black and phase β in white. The grain size α is about 15–20 μm . The chemical composition and mechanical properties are presented respectively in Tables 1 and 2. The core hardness measurement (CHM) was measured in the laboratory and averaged out over 120 measurements that were made in the core of a number of coupons (max = 402.5 HV, min = 305.8 HV, Std. Dev. = 19.24).

2.2 Experimental setup and test conditions

Fatigue failure four-point bending tests were performed on the test coupons shown in Fig. 2. Two chamfers were used to eliminate sharp edges. To finish, they were polished by hand to remove scratches from machining and the concentration of stress generated by the edges of the chamfers. They were taken from the plate so that the stress caused by four-point bending was parallel to the direction T (Fig. 2). The tests were conducted at ambient temperature, with a frequency of 7 Hz and a load ratio $R=0.1$. These tests explored a life cycle domain around 10^5 cycles. Each coupon was milled with a new cutter.

End milling was performed on a 3-axis milling machine of the HURCO brand with a power of 10 kW. The cutting tools used were of the ISCAR brand references ADKT 150524R- HM IC928 and ADKT 150540R-HM IC928, named respectively T1 and T2. These cutters are carbide grade IC928 with a PVD TiAlN coating as recommended for the machining of titanium alloys. These cutters are currently used in the aeronautical industry. The difference between the two cutters lies in the nose radius R_n , which is 2.5 mm for T1 and 4 mm for T2.

Roughness was measured using a Mahr type Perthometer PGK120 roughness meter. Three roughness criteria (ISO 4287) were considered: the arithmetic roughness R_a corresponding to the mean deviation of the profile; roughness R_t , the difference between the maximum height value and the minimum height value within the evaluation length; and roughness R_z , which is the height of irregularities in mean roughness over 10 points.

Measurement of residual stresses (RS) was performed using the X-ray diffraction method (DRX) on a SET-X brand goniometer. Only surface residual stresses were measured, along the feed direction. The residual stresses measured were parallel to the stress induced by the fatigue 4-point bending test.

As far as the metallurgical parameter is concerned, a previous study [21] has highlighted the difficulty involved in measuring microhardness with significant dispersion caused mainly by the very nature of the $\alpha + \beta$ two-phase titanium alloy material. Focusing on the microstructure, no phase change or plastic deformation under the surface was observed. However, the literature [22] reveals the existence of a fine hardened layer very close to the milled surface ($< 10 - 15 \mu\text{m}$). In order to take this into account, a new criterion was sought for the metallurgical parameter with the chord width (noted CW). The diffraction peak (obtained by DRX) allowing the stress condition in a given volume of material to be observed also gives data on the level of dislocations or hardening in it through the width of the diffraction peak or the chord width [23]: the rate of dislocation or hardening increases with an increase in the chord width. Analyses of these peak widths provide a wealth of data and are thus to be studied closely. Recent studies are beginning to study this issue [24, 25].

Roughness and residual stresses were used as a basis to determine the milling plans of the procedure to conduct fatigue tests. To do so, it was decided to correlate low/high roughness values and low/high residual stress values in compression in order to observe their influence on the fatigue lifetime. The chord width was also taken into account. In total six milling plans of procedure were

Table 2 Physical properties of Ti6Al4V alloy

Rm (MPa)	Rp0,2 (MPa)	A (%)	K_{IC} (Mpa \sqrt{m})	ρ (g/cm $^{-3}$)	λ (W.m $^{-1}$ /K $^{-1}$)	CHM (HV)
900–1160	830	8	39	4.43	7	335.65

Fig. 2 Fatigue specimens geometry

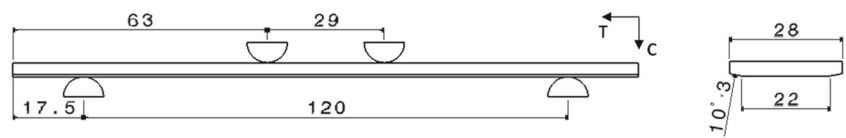


Table 3 Measurement of parameters of surface integrity

Specimen N°	Response				
	Ra (μm)	Rt (μm)	Rz (μm)	RS (MPa)	CW (°)
1	0.312	3.166	1.992	-264	1.819
2	0.684	4.596	3.79	-261	1.991
3	0.38	3.11	2.342	-292	1.794
4	0.412	30.134	2.49	-114	1.406
5	0.47	3.73	3.038	-215	1.282
6	0.528	3.242	2.842	0	1.747

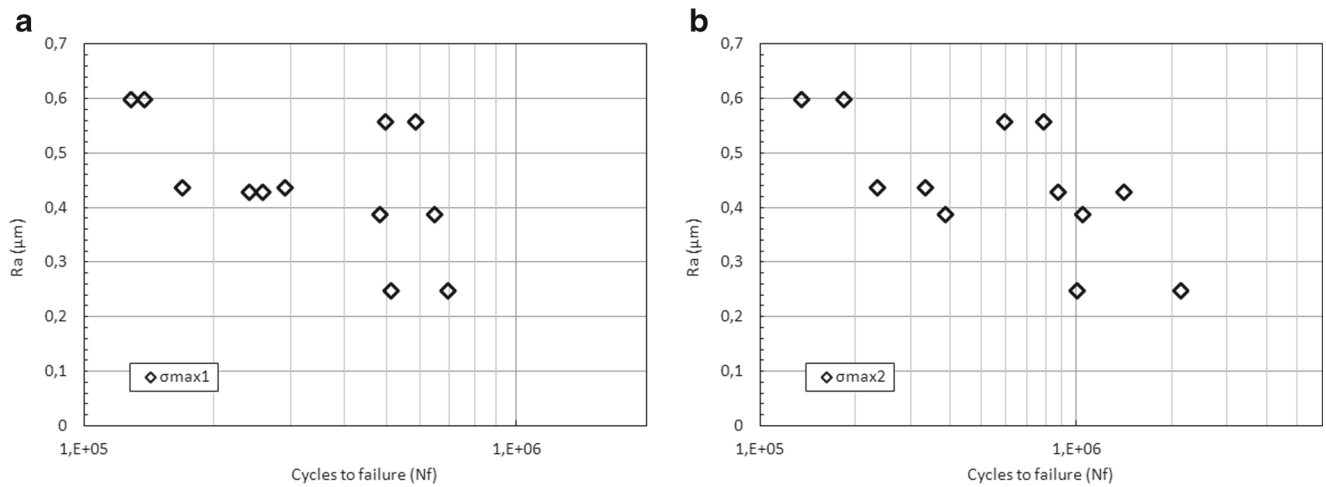


Fig. 3 Roughness Ra depending on the fatigue life time to σ_{max1} and σ_{max2}

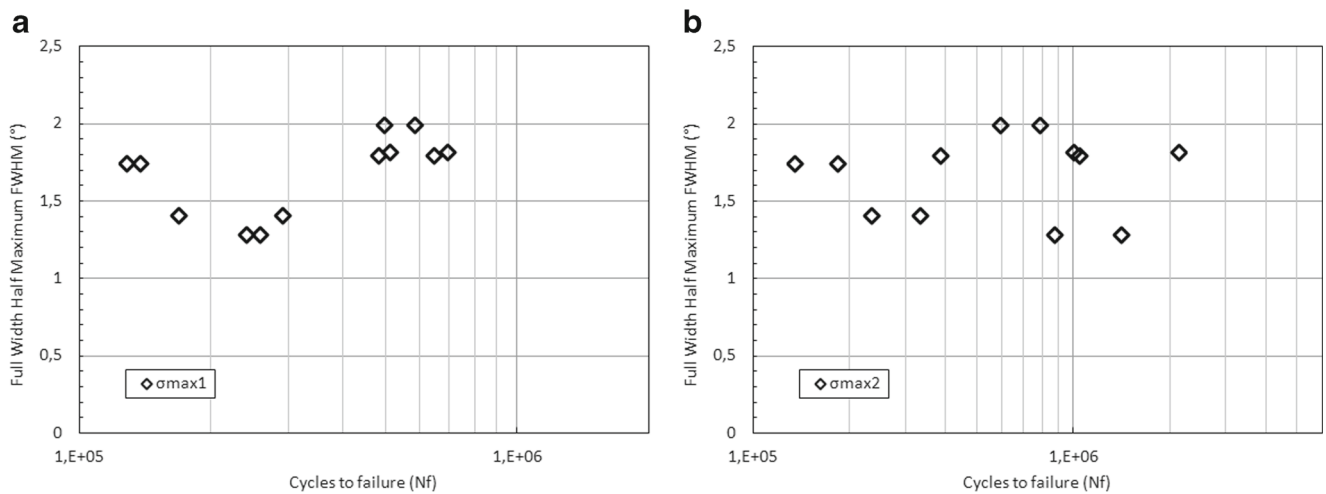


Fig. 4 CW depending on the fatigue life time to σ_{max1} and σ_{max2}

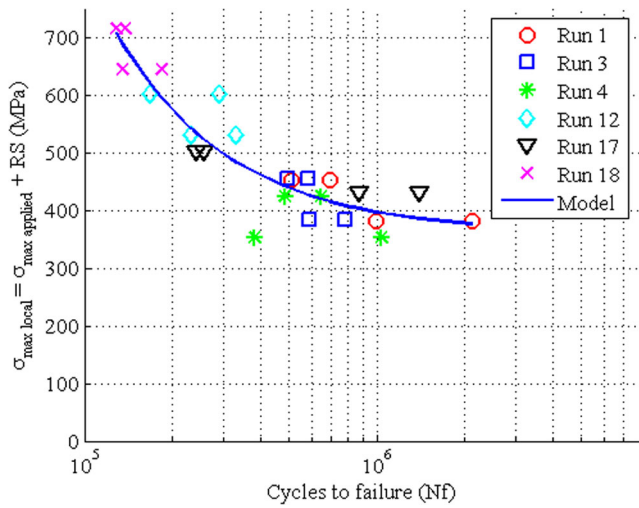


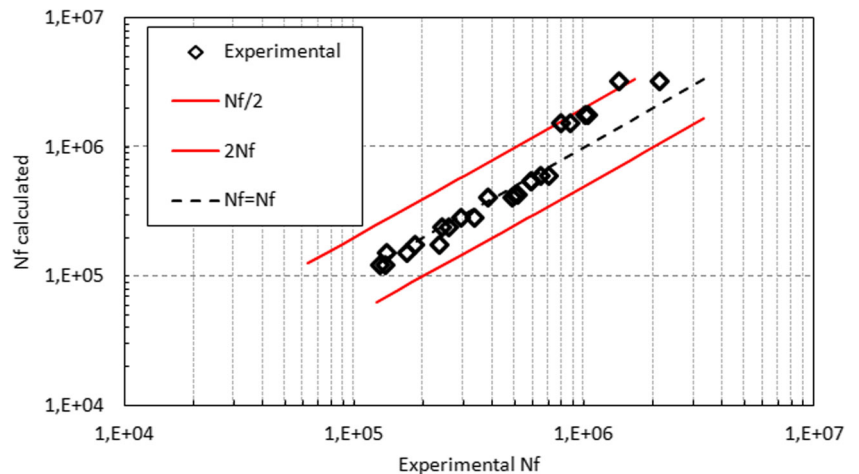
Fig. 5 RS depending on the fatigue life time: $\sigma_{max\ local} = \sigma_{max\ applied} + RS$

retained (Table 3). These were derived from a much broader test campaign. Each plan of procedure was tested for two levels of loading: level 1 (σ_{max1}) and level 2 (σ_{max2}). These were determined in order to obtain a lifetime of between 10^5 and 10^6 cycles. For each level, two coupons were tested. In total, 24 fatigue tests were conducted.

3 Results and discussion

No significant influence of roughness Ra on the fatigue lifetime was observed (Fig. 3). Surfaces with high levels of roughness generated long fatigue lifetimes and for widely differing roughness values very close fatigue lives were also seen. The same observation can be made for Rz and Rt. This tends to prove that roughness does not influence the fatigue lifetime in the present instance.

Fig. 6 Dispersion model based on RS



As for the chord width (CW), there was no observation of a significant effect on the fatigue life (Fig. 4). Indeed, in some cases, low chord widths gave better lifetimes than larger chord widths. Fairly close lifetimes can also be seen with different chord widths.

Conversely, the effect of residual stresses seems to have a preponderant effect on lifetime. Indeed, the more they are subject to compression, the better the lifetime. Pursuing this hypothesis, it was considered that the maximum local stress ($\sigma_{max\ local}$) on the surface could be a good indicator of the effect of the residual stresses. This stress is defined as follows:

$$\sigma_{max\ local} = \sigma_{max\ applied} + RS \tag{1}$$

Measurement values for the residual stresses result from the integral value of stresses over a depth of about $30\ \mu\text{m}$ (depth of penetration of the X-rays). The maximum local stress corresponds to the estimated loading on the volume of material corresponding to that depth.

Figure 5 shows the evolution of this stress corrected according to the fatigue lifetime (Nf). A regrouping of all the experimental points can be seen whatever the milling plan of procedure they represent on a curve. It can also be seen that an asymptote emerges around 380 MPa. A power type law (2) allows this evolution with low dispersion to be described ($R^2 = 0.85$).

$$\sigma_{max\ locale} = 1,535 \times 10^8 Nf^{-1,105} + 362,2 \tag{2}$$

In order to estimate a fatigue model, a logarithmic graph is plotted with Nf calculated as a function of an experimental Nf (Fig. 6). The model is considered to be valid if the experimental points are included between Nf/2 and 2Nf. A good estimation can be seen for shorter lifetimes but as soon as 7.10^5 cycles are exceeded, the model estimates the values less successfully. However, they remain within the tolerance interval.

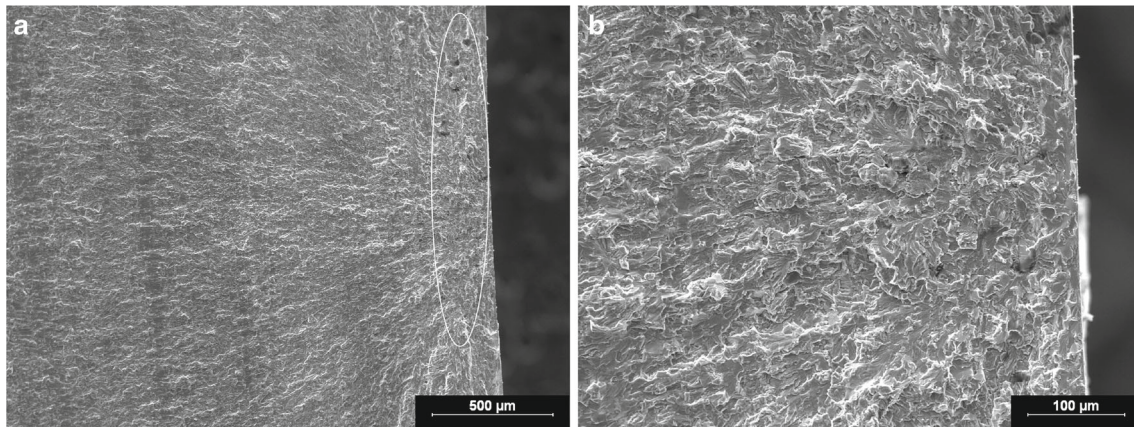


Fig. 7 Fracture morphology of the test 1 σ_{max1} : **a** observation stage I and II, **b** detail of the zone of initiation (stage I)

Figures 7 and 8 show the fracture morphology, observed under the SEM, for two milling plans of procedure: test 1 (long lifetime) and test 6 (short lifetime). On the fractographies, the stage I initiation zone delimited by the white ellipse can be distinguished as can stage II, corresponding to the propagation of long cracks. Stage I is characterised by splitting facets indicating a brittle failure (Figs. 7b and 8b). Stage II also corresponds to splitting. It can be seen that the initiation zone is bigger for the longer lifetimes (high compression residual stresses) than for shorter lifetimes (low compression residual stresses) (Figs. 7a and 8a). No displacement of the zone of initiation at depth was observed in the long and short lifetimes. The breakage mechanisms are the same for all the fatigue test coupons, that is, very close to the surface.

According to the state of the (compressive or tensile) residual stresses, they can either enhance or diminish the fatigue lifetime. Indeed, the test coupons with higher compression residual stresses are associated with the longest fatigue lifetimes. This phenomenon has been observed in other studies [18, 26].

As far as the present study is concerned, residual stresses can modify either the speed of propagation of cracks and/or local loading that is often considered to be an average stress. Over long lifetimes, the initiation period practically overlaps with the lifetime of the coupons. If residual stresses have an effect, it is likely that this will be exerted on initiation. This will mainly consist of a local lowering effect of the mean load. For example, a nominal stress of 700 MPa on a coupon whose residual stresses are -300 MPa will produce the effect on the surface of a maximum load of 400 MPa. The present study's results show such an effect. For short lifetimes, however, the initiation period is short in relation to the propagation period. Propagation models will generally be more appropriate to describe the lifetime. In this case, for the residual stresses to react, they need to slow down propagation of the crack, which is also what is observed in the tests. The effect of the mean load also exists in this instance, but the period of propagation of the crack in the zone subjected to compressive stresses will have to be distinguished from the deeper zone where they disappear. The descriptive model proposed is global for the entire amplitude of

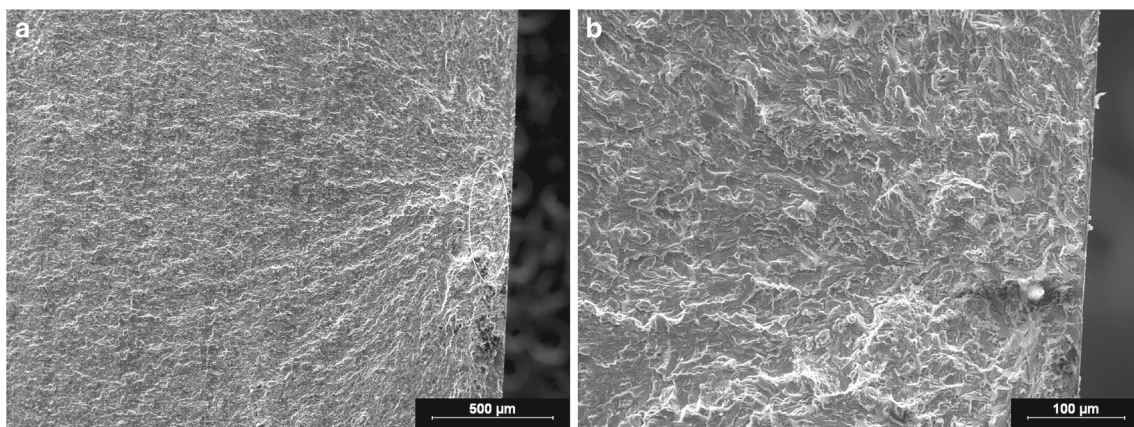


Fig. 8 Fracture morphology of the test 6 σ_{max1} : **a** observation stage I and II, **b** detail of the zone of initiation (stage I)

lifetimes explored and has to be refined to better describe the switch from short to long lifetimes. Even if globally all points of the curve shown in Fig. 6 are within the admitted tolerance band, two zones above and below $7 \cdot 10^5$ cycles can readily be distinguished.

4 Conclusions

The influence of surface integrity on fatigue lifetime was studied. The conclusion that can be drawn from the results is as follows:

- the geometric (roughness) and metallurgical (chord width) parameters appear not to influence fatigue lifetime, while the mechanical parameter (residual stresses) does indeed seem to be determinant.
- A regrouping of all the experimental points can be seen whatever the milling plan of procedure they represent on a curve. The residual stresses appear to provide the best indicators, especially those in compression through their modifying the local load of the test coupon surface. Compressive residual stresses are beneficial to the fatigue lifetime.
- A phenomenological model was proposed that provides an appropriate description of fatigue behaviour. A good estimation can be seen for shorter lifetimes but as soon as $7 \cdot 10^5$ cycles are exceeded, the model estimates the values less successfully but always in the tolerance interval.
- It can be seen that the initiation zone is bigger for the longer lifetimes (high compression residual stresses) than for shorter lifetimes (low compression residual stresses). It was also noted that the failure mechanisms were qualitatively identical over all the fatigue test coupons; each initiation was very close to the surface.

Acknowledgements The authors would like to acknowledge Airbus Toulouse for providing the material and tools in this work.

References

1. Novovic D, Dewes RC, Aspinwall DK, Voice W, Bowen P (2004) *Int J Machine Tools Manufac* 44(2-3):125. doi:10.1016/j.ijmachtools.2003.10.018
2. Ezugwu E (2005) *Int J Machine Tools Manufac* 45(12-13):1353. doi:10.1016/j.ijmachtools.2005.02.003
3. KONIG W (1978) Proceedings of 47th Meeting of AGARD Structural and Materials Panel. Florence, Italy, pp 1.1–1.10
4. Sun J, Guo Y (2008) *Int J Machine Tools Manufac* 48(12-13):1486. doi:10.1016/j.ijmachtools.2008.04.002
5. Ezugwu EO, Wang ZM (1997) *J Mater Process Technol* 68(3):262. doi:10.1016/S0924-0136(96)00030-1
6. Suraratchai M, Limido J, Mabru C, Chieragatti R (2008) *Int J Fatigue* 30(12):2119. doi:10.1016/j.ijfatigue.2008.06.003
7. Shahzad M, Chaussumier M, Chieragatti R, Mabru C, Aria FR (2010) *J Mater Process Technol* 210(13):1821. doi:10.1016/j.jmatprotec.2010.06.019
8. Gaceb M, Brahmi S (2007) Etude de l'influence de l'état de surface sur la tenue à la fatigue d'un acier XC48 (Laboratoire de Fiabilité des Equipements Pétroliers et matériaux, Université M'Hamed Bougara de Boumerdes Algérie)
9. Schwach DW, Guo Y (2006) *Int J Fatigue* 28(12):1838. doi:10.1016/j.ijfatigue.2005.12.002
10. Sharman ARC, Aspinwall DK, Dewes RC, Clifton D, Bowen P (2001) *Int J Machine Tools Manufac* 41(11):1681. doi:10.1016/S0890-6955(01)00034-7
11. Flavenot J, Skalli N, Maitre FL (1983) *CIRP Ann - Manufac Technol* 32(1):475. doi:10.1016/S0007-8506(07)63443-X
12. Elkhabeery MM, Fattouh M (1989) *Int J Machine Tools Manufac* 29:391
13. Lieurade HP (1989) *Surfaces* 27(206):87
14. Wagner L, Lutjering G (1981)
15. Mitryaev KF, Seryapin YA (1984) *Soviet Eng Res* 4:17
16. Wagner L (1999) *Mater Sci Eng A* 263(2):210. doi:10.1016/S0921-5093(98)01168-X
17. Ludian T, Wagner L (2008) *Adv Mater Sci* 8(2):44. doi:10.2478/v10077-008-0030-5
18. Smith S, Melkote SN, Lara-Curzio E, Watkins TR, Allard L, Riester L (2007) *Mater Sci Eng A* 459(1-2):337. doi:10.1016/j.msea.2007.01.011
19. Welsch G, Boyer R, Collings EW (1994) *Materials properties handbook: Titanium alloys*, (ASM. International)
20. Combres Y (1999) *Propriétés du titane et de ses alliages (Techniques de l'ingénieur M557)*
21. Moussaoui K, Mousseigne M, Senatore J, Chieragatti R, Monies F *The International Journal of Advanced Manufacturing Technology*, pp 1–13. doi:10.1007/s00170-012-4582-5
22. Velasquez JDP (2007) Etude des copeaux et de l'intégrité de surface en usinage à grande vitesse de l'alliage de titane TA6V. Ph.D. thesis. Université Paul Verlaine Metz
23. Castex L, Lebrun JL, Maeder G, Sprauel JM (1981) Détermination des contraintes résiduelles par diffraction des rayons X. No. 22 in *Publications scientifiques et techniques - Ecole nationale supérieure d'arts et métiers, ISSN 0768-1429 ENSAM. France, Paris*
24. Hoffmeister J, Schulze V, Hessert R, Koenig G (2012) *Int J Mater Res* 103(1):66. doi:10.3139/146.110630
25. Madariaga A, Esnaola JA, Fernandez E, Arrazola PJ, Garay A, Morel F (2013) *The International Journal of Advanced Manufacturing Technology*, pp 1–12. doi:10.1007/s00170-013-5585-6
26. Javidi A, Rieger U, Eichlseder W (2008) *Int J Fatigue* 30(11):2050. doi:10.1016/j.ijfatigue.2008.01.005